

1 **Title**

2 Variable impact of wildfire smoke on ecosystem metabolic rates in lakes

3 **Running Head**

4 Smoke affects lake metabolism

5 **Authors**

6 Adrienne P. Smits*¹, Facundo Scordo^{2,3†,4†}, Minmeng Tang^{5,6†}, Alicia Cortés^{7,9}, Mary Jade
7 Farruggia¹, Joshua Culpepper^{8†}, Sudeep Chandra², Yufang Jin⁵, Sergio A. Valbuena^{7,9}, Shohei
8 Watanabe⁹, Geoff Schladow^{7,9}, Steven Sadro¹

9 **Affiliations**

10 ¹ Environmental Science and Policy, University of California Davis, Davis, CA, USA;

11 asmits@ucdavis.edu

12 ² Department of Biology, University of Nevada Reno, Reno, NV, USA

13 ³ Instituto Argentino de Oceanografía, Universidad Nacional del Sur (UNS)-CONICET, Bahía
14 Blanca, Buenos Aires, Argentina

15 ⁴ Departamento de Geografía y Turismo, Universidad Nacional del Sur, Bahía Blanca, Buenos
16 Aires, Argentina

17 ⁵ Land, Air, and Water Resources, University of California Davis, Davis, CA, USA

18 ⁶ Civil and Environmental Engineering, Cornell University, Ithaca, NY, USA

19 ⁷ Civil and Environmental Engineering, University of California Davis, Davis, CA, USA;

20 ⁸ Department of Biology, York University, Toronto, ON, Canada;

21 ⁹ Tahoe Environmental Research Center, University of California Davis, Davis, CA, USA

22 ***This manuscript is a non-peer-reviewed preprint submitted to EarthArXiv. This**
23 **manuscript has also been submitted to Global Change Biology for peer-review.***

24

25

26

27

28

29

30

31

32

33

34

35

36 **Abstract**

37 Increasingly severe wildfires release smoke plumes that cover entire continents, depositing
38 aerosols and reducing solar radiation fluxes to millions of freshwater ecosystems, yet little is
39 known about their impacts on inland waters. This large scale study 1) quantified annual and
40 seasonal trends in the spatial extent of dense smoke cover in California, USA, over the last 18
41 years (2006 - 2022), and 2) assessed the impacts of dense smoke cover on daily gross primary
42 production (GPP) and ecosystem respiration (R) in 10 lakes spanning a large gradient in nutrient
43 concentration and water clarity, during the three smokiest years in our dataset (2018, 2020,
44 2021). We found that the maximum spatial extent of dense smoke cover between June-October
45 has increased to 70% of California's area since 2006, with the greatest increases in August and
46 September. In the three smokiest years, lakes were exposed to an average of 33 days of dense
47 smoke between July and October, resulting in substantial reductions in shortwave radiation
48 fluxes and 3 to 4-fold increases in atmospheric fine particulate matter concentrations (PM_{2.5}).
49 However, responses of lake GPP to smoke cover were extremely variable among and within
50 lakes, as well as between years. In contrast, the response of rates of ecosystem respiration to
51 smoke was related to lake nutrient concentrations and water temperature –respiration rates
52 decreased during smoke cover in cold, oligotrophic lakes but not in warm, eutrophic lakes. The
53 impacts of dense, prolonged smoke cover on inland waters are likely to be highly variable within
54 and among regions due to mediating effects of lake attributes and seasonal timing of wildfires.

55 **Key Words**

56 Wildfire, smoke, lakes, ecosystem metabolism, primary productivity, respiration, nutrients,
57 shortwave radiation

58 **Introduction**

59 Increasingly frequent and severe wildfires associated with climate change release vast quantities
60 of smoke into the atmosphere¹, generating plumes that travel thousands of kilometers² and
61 expose millions of water bodies to smoke for weeks to months³. Aerosols within smoke plumes
62 absorb or scatter solar radiation⁴, reducing total fluxes to terrestrial and aquatic ecosystems and
63 altering the spectral composition of light. Smoke aerosol particles also contain carbon and
64 nutrients such as phosphorus (P) and nitrogen (N), which can fertilize receiving ecosystems^{5,6}.
65 Both reduced solar radiation and particle deposition affect physical and biological processes in
66 aquatic ecosystems, for example by reducing water temperature⁷ or altering rates of gross
67 primary production (GPP) and ecosystem respiration (R)⁸. Changes in ecosystem metabolic rates
68 can alter critical ecosystem processes such as carbon and nutrient cycling, rates of carbon burial
69 and greenhouse gas emission, and food web structure⁹. Currently, little is known about how
70 ecosystem metabolic rates may respond to wildfire smoke in lakes spanning gradients in size or
71 productivity.

72 Smoke effects on ecosystem metabolic rates (i.e., GPP or R) have rarely been measured, despite
73 the increased exposure of ecosystems to high-density smoke³. To date, studies of smoke impacts
74 on ecosystems focus primarily on the effects of altered radiation fluxes to forest or cropland
75 production^{10–12}, or on the effects of aerosol deposition on phytoplankton growth in oligotrophic
76 marine systems^{6,13,14}. Existing studies of smoke effects on inland waters are limited to single site
77 case studies (e.g., Castle Lake^{8,15}; Lake Tahoe¹⁶) or focus on relatively few response variables
78 (e.g., water temperature⁷, cyanobacterial blooms¹⁷). The influence of smoke cover on freshwater
79 ecosystems at spatial scales greater than single sites is not yet understood but is of growing
80 importance, as wildfires release smoke across whole continents¹⁸. A lack of regional-scale

81 studies limits understanding of variability in lake responses or its causes. While the influence of
82 smoke cover on aquatic systems was first described decades ago¹⁶, limnological research has not
83 kept pace as wildfire smoke becomes a global rather than local phenomenon.

84 While the effects of smoke on ecosystem rates of primary production and respiration have rarely
85 been explored, the roles of light, temperature, and nutrients in regulating ecosystem metabolic
86 rates have a strong theoretical underpinning and long history of empirical study^{19,20}. Predicting
87 ecosystem responses to smoke relies on understanding how the relative importance of different
88 drivers varies across ecosystems or through time within individual systems. For example, the
89 same reduction in photosynthetically active radiation (PAR) due to smoke might reduce rates of
90 primary production in a eutrophic lake where phytoplankton are light-limited but increase rates
91 of production in a clear-water lake where phytoplankton are photo-inhibited (Figure 1a).

92 Likewise, the effect of aerosol deposition on ecosystem metabolic rates (i.e., the fertilization
93 effect) depends on the concentration and nutrient stoichiometry of smoke particulates³, as well as
94 on ambient nutrient concentrations within lakes (Figure 1c). In contrast, reduced water
95 temperature due to smoke cover should decrease ecosystem metabolic rates across all systems,
96 dependent on the temperature coefficient (Q_{10} ; Figure 1b). The few existing studies of smoke
97 effects on ecosystem metabolic rates illustrate high variability in responses in both terrestrial and
98 aquatic systems. In a forest where smoke cover decreased total PAR fluxes, GPP was reduced at
99 the leaf scale but increased at the canopy scale because smoke increased diffuse PAR and
100 illuminated a greater proportion of the canopy¹⁰. Likewise, while GPP increased during smoke
101 cover in surface waters within a mesotrophic lake, it declined deeper in the water column where
102 phytoplankton were light-limited⁸. How individual ecosystems respond to smoke will

103 consequently depend on both how smoke affects fundamental drivers (light, temperature,
104 nutrients) and on system-specific attributes such as water clarity and nutrient concentrations.
105 Here we present the first regional investigation of the effects of smoke exposure on ecosystem
106 metabolic rates in inland waters. First, we quantified annual and seasonal trends in the spatial
107 extent of medium and high-density smoke cover (hereafter ‘med-high density’) in California,
108 USA, over 18 years (2006 - 2022) using remote sensing. We then asked the following broad
109 questions: 1) Are responses of ecosystem metabolism to smoke uniform across different types of
110 lakes? 2) Do smoke density, duration, or seasonal timing influence how ecosystems respond?
111 and 3) to what extent are responses in GPP and R to smoke coupled or decoupled?

112 To address these questions, we quantified changes in daily shortwave radiation (SW),
113 atmospheric fine particulate matter concentrations (PM_{2.5}), water temperature, and ecosystem
114 metabolism during periods of med-high density smoke cover in 9 freshwater lakes and one
115 freshwater tidal slough in California (Figure 2a, Table 1), where wildfire extent has increased
116 five-fold since the 1970s²¹. We measured responses to smoke in 2018, 2020, and 2021, the three
117 worst fire seasons on record in California²². We estimated rates of ecosystem metabolism from
118 hourly dissolved oxygen (DO) measurements in both pelagic (open-water) and littoral (near-
119 shore) environments within study sites (total = 22 datasets). Study sites spanned wide ranges in
120 nutrient availability, water clarity, and size, from ultra-oligotrophic (e.g., Lake Tahoe) to hyper-
121 eutrophic (e.g., Clear Lake).

122 We hypothesized that ecosystem metabolic responses to smoke would vary primarily in relation
123 to water clarity and organic matter and nutrient availability, with GPP and R tending to increase
124 in the surface waters of oligotrophic systems but decrease in meso- or eutrophic-systems. We

125 expected to see greater changes in metabolism during dense, prolonged smoke cover compared
126 to short, intermittent smoke events. Finally, we expected the magnitude of change in GPP and R
127 to be coupled in oligotrophic systems, where available carbon pools are lower and respiration is
128 primarily fueled by recent autochthonous production²³. However, we expected GPP and R would
129 be decoupled in more productive systems, where high organic matter (OM) and nutrient
130 concentrations fuel respiration by heterotrophs irrespective of changes in GPP²⁴.

131 **Methods**

132 *Study sites and in-situ data collection*

133 We collected continuous hourly DO and water temperature data from 10 water bodies distributed
134 across the northern two-thirds of California, USA, from June-October in 2018, 2020, and 2021
135 (Table 1; Figure 2). Study sites are located in several of the major mountain ranges in California,
136 including the southern Sierra Nevada (5 sites; ‘Sequoia lakes’), northern Sierra Nevada (2 sites;
137 Lake Tahoe and Dulzura Lake; ‘Tahoe lakes’), Klamath Mountains (1 site; Castle Lake), and
138 northern Coast Range mountains (1 site; Clear Lake), as well as within the Sacramento-San
139 Joaquin River Delta (1 site; Delta). Sites span large gradients in elevation (0 - 3200 m.a.s.l), size
140 (0.2 - 49624 ha), water clarity (k_d 0.09 - 2 m⁻¹), and trophic status (ultra-oligotrophic -
141 hypereutrophic; Table 1).

142 Water bodies were instrumented with continuous in situ DO and temperature sensors at 1-2
143 locations per site (14 total). In 7 sites (Sequoia lakes, Clear Lake, and Delta), DO and
144 temperature were measured only in pelagic (mid-lake) habitats. In two lakes (Castle, Dulzura),
145 DO and temperature were measured in both pelagic and littoral habitats. In Lake Tahoe, DO and
146 temperature were only measured in two littoral sites. For all lakes, DO and temperature data

147 were only available for a subset of the three study years (Table 1). In addition to hourly sensor
148 data, for each lake and year we obtained water chemistry data collected from lake surface waters
149 (0- 3 m depth) between June 1 and November 1, for the following constituents: chlorophyll-a
150 concentration ($\mu\text{g L}^{-1}$), total dissolved phosphorus (TDP; $\mu\text{g L}^{-1}$), and total dissolved nitrogen
151 (TDN; $\mu\text{g L}^{-1}$). Water chemistry data were used to classify lake trophic status but were not
152 collected at sufficient temporal resolution to evaluate changes associated with smoke cover.

153 Meteorological data corresponding to time periods of in-situ sensor data collection were obtained
154 for each lake from the nearest available weather station (SW radiation, W m^{-2} ; wind speed, m s^{-1} ;
155 air temperature, $^{\circ}\text{C}$). We also obtained mean daily atmospheric fine particulate matter
156 concentrations ($< 2.5 \mu\text{m}$ in diameter; PM2.5; $\mu\text{g m}^{-3}$) from the nearest PurpleAir or EPA sensor.
157 No PM2.5 data are available for the Sequoia Lakes in 2020. In total, we compiled 22 hourly DO
158 and water temperature datasets, 9 corresponding hourly meteorological datasets, 8 daily PM2.5
159 datasets, and 19 water chemistry datasets (detailed site and dataset descriptions can be found in
160 Supplementary Methods).

161 *Quantifying patterns and trends in California smoke cover*

162 We used the smoke plume product from the NOAA/NESDIS Satellite Analysis Branch's Hazard
163 Mapping System (HMS)³⁸, to quantify the spatial and temporal patterns of smoke cover in
164 California from 2006 to 2022. This product provides a daily smoke plume density polygon over
165 North America at a 4 km resolution by integrating near real-time polar-orbiting and
166 geostationary satellite imagery from Geostationary Operational Environmental Satellite Program
167 (GOES), Moderate Resolution Imaging Spectroradiometer (MODIS), and Advanced Very High
168 Resolution Radiometer (AVHRR). This remote sensing product classified smoke plumes into

169 three categories: low, medium, and high density, based on the estimated smoke concentrations of
170 5, 16, 27 $\mu\text{g m}^{-3}$, respectively.

171 To quantify the spatial extent and duration of smoke cover in California for each year, we made
172 an annual composite map of smoke cover by intersecting daily smoke plume polygons with each
173 intersecting polygon recording the number of smoke days for a given year. All areas exposed to
174 smoke for at least one day were then summarized to quantify the annual spatial extent of smoke
175 cover. This process was repeated for each month to evaluate the seasonal and interannual
176 patterns of smoke cover extent in California, for each smoke density. In further analyses, we
177 focused on medium and high-density smoke cover (hereafter ‘med-high density’) rather than low
178 density smoke cover because we assumed more dense smoke cover would be of greater
179 ecological relevance (e.g., more likely to reduce SW radiation fluxes and deposit particulates into
180 lakes).

181 We assessed time series of maximum med-high density smoke cover extent in the months June-
182 October, as well as annual and seasonal means, for monotonic trends by computing Sen’s slopes
183 and applying the Mann-Kendall test using the ‘wql’ package in R³⁹.

184 In addition to quantifying smoke cover throughout California, we generated a daily smoke
185 density sequence over each study lake from 2006 - 2022. First, we obtained lake shapefiles from
186 the California Lake database maintained by California Department of Fish and Wildlife
187 (CDFW)⁴⁰. For study sites that were not included in the California Lake database (e.g., small
188 ponds in Sequoia National Park), we used a 100 meter buffer around the central point in the lake
189 as an approximation of the lake surface. We then assigned a daily smoke density value to each
190 lake by comparing spatial relationships between smoke plume polygons and lake surfaces. If a

191 smoke plume intersected a lake's surface area, we assigned the corresponding smoke density to
192 the lake based on the date. If multiple smoke densities were assigned to the same lake on the
193 same date, only the highest smoke density was assigned.

194 *Characterizing lake exposure to smoke during study period*

195 We identified periods of smoke cover for each lake during the study years (2018, 2020, 2021)
196 using a combination of the daily smoke density value (described in previous section), SW
197 radiation measurements from weather stations, PM_{2.5} concentrations, and visual inspection of
198 Sentinel satellite images to confirm the presence of smoke plumes.

199 We classified each day as 'smoke' or 'non-smoke' as follows: we modeled theoretical 'clear-
200 sky' SW radiation ($SW_{\text{clear.sky}}$) for each day using a statistical clear sky algorithm⁴¹. We then
201 subtracted the measured daily mean SW (SW_{meas}) from $SW_{\text{clear.sky}}$ ($SW_{\text{diff}} = SW_{\text{clear.sky}} - SW_{\text{meas}}$).
202 We calculated the median value of SW_{diff} on days with smoke density of zero across all 9
203 meteorological datasets (median $SW_{\text{diff}} = 20 \text{ W m}^{-2}$). Days were conservatively classified as
204 smoke days if they met two conditions: 1) daily mean SW radiation was reduced by more than
205 20 W m^{-2} and 2) smoke density was medium or high.

206 For each lake-year combination, we characterized the following attributes of smoke exposure: 1)
207 the total number of smoke days between July 1-Oct 1; 2) the intermittence of smoke cover,
208 defined as the mean, median, and maximum number of consecutive smoke days that occurred in
209 each dataset; and 3) the cumulative reduction in SW radiation relative to clear sky values on
210 smoke days ('cumulative SW deficit'). We calculated cumulative SW deficit by summing SW_{diff}
211 on all smoke days between July 1 and October 1, when the majority of smoke days occurred.

212 Attributes of smoke cover were only quantified between July 1 - October 1 because some
213 datasets were incomplete outside this seasonal window.

214 *Estimating aquatic ecosystem metabolic rates*

215 We modeled daily rates of gross primary production (GPP; mg DO L⁻¹ d⁻¹), ecosystem
216 respiration (R), and net ecosystem production (NEP = GPP - R) in the surface mixed layer of our
217 study sites using hourly DO (mg L⁻¹), water temperature (° C), PAR (μmol m⁻² s⁻¹), and wind
218 speed (m s⁻¹) measurements using the Lake Metabolizer R package⁴². For pelagic sites in lakes
219 that stratified seasonally or periodically (Emerald Lake, Topaz Lake, Castle Lake, Clear Lake)
220 we estimated metabolic rates in the surface mixed layer. We calculated mixed layer depth (Z_{mix})
221 using depth-distributed water temperature measurements from fixed depth sensors or vertical
222 profiles using LakeAnalyzer in R⁴³. For littoral sites within stratified lakes (Castle Lake, Dulzura
223 Lake, Lake Tahoe), and in small, shallow water bodies that did not stratify (TOK 11 Pond, EML
224 Pond 1, Topaz Pond), Z_{mix} was set to lake depth at the location of the DO sensor. In the tidally-
225 influenced Delta, Z_{mix} was set to the mean depth of the channel within the range of the tidal
226 excursion (see Supplementary Methods for details on data used in metabolism models).

227 To estimate oxygen fluxes across the air-water interface, we used a wind-based gas exchange
228 model that accounted for lake surface area⁴⁴. We set gas exchange to zero during periods when
229 the DO sensor was below the diel thermocline. We estimated average PAR within the surface
230 mixed layer by converting shortwave radiation measurements from weather stations to surface
231 PAR and then using the attenuation coefficient for PAR (k_d ; m⁻¹ Table 1) and Z_{mix} to estimate
232 mean water column PAR as in Staehr et al⁴⁵. Days with unrealistic metabolism estimates
233 (negative GPP, positive R) were excluded from results.

234 *Quantifying effects of smoke cover on ecosystem metabolic rates*

235 We quantified ecosystem metabolic responses to smoke cover (e.g., compared GPP, R, and NEP
236 between smoke and non-smoke days) by fitting generalized additive mixed models (GAMMs) to
237 the data using the ‘mgcv’ R package⁴⁶. To facilitate comparisons across sites spanning from
238 hyper-eutrophic (Clear Lake) to ultra-oligotrophic (Lake Tahoe), we first standardized
239 metabolism time series by mean and variance (z-score). We modeled daily metabolic estimates
240 as a function of smoke cover (categorical: smoke or non-smoke) and day of year (doy; smooth
241 term). We included an interaction between the smooth function of doy and smoke (e.g.,
242 estimated separate seasonal smooths for non-smoke and smoke days) in order to visualize the
243 effect of smoke cover on seasonal patterns in metabolism. We included a random effect of site in
244 all models to account for the non-independence of repeated measurements in each lake. GAMM
245 models were fitted using default thin plate regression splines for the smooth terms.

246 **Results**

247 *Increased spatial extent and duration of medium-high density smoke in California since 2006*

248 Over the last 18 years (2006 - 2022), the months July, August, and September had the greatest
249 maximum spatial extent of med-high density smoke cover in California (maximum coverage >
250 40%; Figure 2b), followed by June (30%) and October (18%). Two of the main study years
251 (2020, 2021) were outliers in the seasonal timing of smoke cover: the maximum extent of med-
252 high density smoke exceeded 70% of California in September and October in both years (Figure
253 2b red points in boxplot; Supplementary Figure 1).

254

255 From 2006 to 2022, the maximum extent of med-high density smoke increased significantly in
256 every month between June and October. Maximum smoke extent increased the fastest in August
257 (23,360 km² year⁻¹ or 5.5% of California's area year⁻¹, Kendall's S = 68, p = 0.005, n=18) and
258 September (20,392 km² or 4.8% year⁻¹, S=80, p=0.001), followed by July (16,704 km² or 3.9%
259 year⁻¹, S = 67, p = 0.006). Averaged across the predominant smoke season (June - October), the
260 maximum extent of med-high density smoke cover has increased by ~300,000 km², or 70% of
261 California's area, over the last 18 years (S = 83, p = 0.0007; dashed line in Figure 2c). Our study
262 years (2018, 2020, 2021) had the greatest spatial extent of med-high density smoke since 2006
263 (Figure 2c).

264

265 The duration of med-high density smoke cover at the 10 study sites was highly variable among
266 years but increased dramatically during the study years (Figure 2d). From 2006 - 2022, sites
267 experienced an average of 15 med-high density smoke days per year (range 0 - 69 days). There
268 were regional differences in smoke duration between the study years (2018 - 2021; Figure 2a),
269 likely related to proximity to wildfires and prevailing wind patterns. For example, in 2021 smoke
270 affected the northern Sierra Nevada mountains, Klamath mountains and Sacramento Delta more
271 than the southern Sierra Nevada mountains.

272

273 *Variable lake exposure to smoke (2018, 2020, 2021)*

274 Across all site-year combinations where independent meteorological data were available (n =
275 1043 days), daily mean SW radiation fluxes on smoke days were significantly less than those on
276 non-smoke days (205 versus 254 W m⁻²; t = -11.613, p < 2.2 x 10⁻¹⁶, df = 888.97; Figure 3a), a
277 reduction of 20% relative to clear-sky estimates (SW_{diff} = mean reduction 57 W m⁻²; n = 394).

278 Atmospheric PM_{2.5} concentrations were elevated on smoke days compared with non-smoke
279 days (92 versus 17 $\mu\text{g m}^{-3}$; $t = 11.411$, $p < 2.2 \times 10^{-16}$, $df = 306.31$; Figure 3b).

280

281 Exposure to smoke varied in duration, intermittence, and intensity across the 9 meteorological
282 datasets (Table 2). During the three study years (2018, 2020, 2021) study sites experienced an
283 average of 33 smoke days between July 1 and Oct 1 (range 23 - 45 days; Table 2). The timing of
284 smoke events varied among sites and years, but in general August and September had more
285 smoke days than July (mean of 14 days versus 3 days), matching the results from the 18-year
286 smoke time series (Figure 2b). The mean length of smoke events (consecutive smoke days)
287 ranged from 3 - 8 days, but there was large variation in the maximum length of smoke events
288 across the datasets (4 - 21 days; Table 2). The cumulative deficit in SW fluxes due to smoke
289 (e.g., smoke intensity; 10^6 J m^{-2}) varied three-fold among lake-years, with the greatest SW
290 reductions at Emerald Lake (2020, 2021) and Lake Tahoe (2021) and the least at Castle Lake in
291 2018 (Table 2; Figure 3c-d).

292 *Responses of ecosystem metabolism to smoke*

293 Rates of ecosystem metabolism were highly variable among the 10 sites and were temporally and
294 spatially variable within lakes (Supplementary Table 1, Supplementary Figures 2, 3). Volumetric
295 rates of GPP in pelagic habitats ranged from $0.11 \pm 0.09 \text{ mg DO L}^{-1} \text{ d}^{-1}$ in oligotrophic Emerald
296 Lake to $1.43 \pm 1.26 \text{ mg DO L}^{-1} \text{ d}^{-1}$ in hyper-eutrophic Clear Lake. Littoral habitats and shallow
297 ponds tended to have higher volumetric rates of GPP than pelagic sites or deeper lakes, ranging
298 from $0.59 \pm 0.16 \text{ mg DO L}^{-1} \text{ d}^{-1}$ in TOK 11 Pond to $1.62 \pm 0.30 \text{ mg DO L}^{-1} \text{ d}^{-1}$ in Dulzura Lake.
299 In Castle and Dulzura, where we estimated metabolism in both pelagic and littoral habitats, mean
300 rates of GPP in littoral areas were >3 times the corresponding rates in mid-lake surface water

301 (Supplementary Table 1). Sites with warmer water temperatures and higher chlorophyll-a (chl_a),
302 total dissolved N (TDN), and total dissolved P (TDP) concentrations had higher rates of GPP
303 (see Supplementary Table 2 for water chemistry summary; Supplementary Table 3 for
304 correlation matrix). Respiration rates were strongly correlated with GPP overall (Pearson's $r =$
305 0.94 , $n = 1772$ metabolism days), though the strength of this correlation varied considerably
306 among datasets ($0.34 - 0.96$; Table S1). Similar to GPP, R was highest in warm lakes with higher
307 chlorophyll-a (chl_a) and nutrient concentrations (e.g., Delta and Clear Lake). Mean NEP was
308 negative in 18 out of 22 datasets; only 3 littoral sites (Castle Lake, Dulzura Lake, and Lake
309 Tahoe) and one pelagic site (Castle Lake) had positive mean NEP.

310

311 Rates of GPP (z-scored) were significantly lower on smoke days than on non-smoke days
312 (GAMMs: parametric effect = -0.22 ± 0.05 (SE), $p = 1.97 \times 10^{-5}$, $n = 1772$; Figure 4a). Though
313 GPP declined seasonally, smoke cover further reduced rates relative to the seasonal decline
314 (Figure 4d). Median GPP was lower during smoke days in most of the datasets (negative Δ GPP;
315 Figure 4g), decreasing by up to 70% in Clear Lake (OA) in 2020. However, median GPP
316 was higher in certain sites and years, increasing by up to 50% in the littoral zone of Lake Tahoe
317 in 2021 (Extended Data Figure 3; Supplementary Table 1). Respiration rates were lower on
318 smoke days (effect = -0.24 ± 0.05 , $p = 5.64 \times 10^{-7}$, $n = 1772$, Figure 4b), and smoke cover
319 accelerated seasonal declines in R (Figure 4e). Median rates of R were up to 52% lower during
320 smoke days (EML Pond 1 in 2021). Only mesotrophic or eutrophic sites showed higher median
321 rates of R during smoke days (positive Δ R; Figure 4h), increasing by up to 44 % in Clear Lake
322 (OA) in 2021. Unlike GPP and R, NEP was not significantly different between smoke and non-
323 smoke days across all the datasets (effect = 0.03 ± 0.05 , $p = 0.60$; Figure 4c, f). NEP tended to be

324 more positive on smoke days in oligotrophic sites and more negative in mesotrophic or eutrophic
325 sites (Figure 4i).

326

327 Because GPP and R were coupled in most sites, responses of GPP and R to smoke (Δ GPP, Δ R)
328 were also positively correlated (Figure 5a; effect = 0.52 ± 0.16 , $R^2 = 0.30$, $p = 0.005$, $n = 22$).

329 However, no lake attribute or smoke variables explained GPP responses to smoke; Δ GPP was
330 not related to log-TDP (Figure 5b; $p = 0.43$), log-TDN ($p = 0.37$), log-chla ($p = 0.69$), mean

331 summer water temperature ($p = 0.36$), or other site or smoke variables (Supplementary Table 3).

332 In contrast, Δ R was positively correlated with site variables such as mean summer water
333 temperature (effect = 0.09 ± 0.02 , $R^2=0.38$; $p = 0.0012$), log-TDP (Figure 5c; effect 0.19 ± 0.04 ,

334 $R^2 = 0.41$, $p = 0.00073$), log-TDN (effect 0.45 ± 0.13 , $R^2 = 0.33$, $p = 0.003$), and log-chla (effect
335 0.22 ± 0.05 , $R^2 = 0.39$, $p = 0.001$); respiration rates were lower on smoke days in cold, low-

336 nutrient lakes. R was also reduced in sites that experienced more prolonged smoke cover

337 (number of smoke days; effect = -0.04 ± 0.015 , $R^2 = 0.27$, $p = 0.007$) and greater smoke intensity
338 (higher SW deficit, 10^6 J m^{-2} ; effect = -0.0005 ± 0.0001 , $R^2 = 0.40$, $p = 0.0008$). However,

339 because the oligotrophic lakes in the Tahoe basin and Sequoia National Park were also exposed
340 to more prolonged and high-density smoke than the mesotrophic and eutrophic sites (Table 2;

341 Figure 3c-d), we were not able to robustly distinguish the effects of smoke exposure attributes
342 and lake variables on metabolic responses. Though littoral and pelagic habitats within the same

343 water bodies responded differently to smoke cover, across sites there were no consistent

344 differences in metabolic responses between the two habitat types.

345

346 **Discussion**

347 *Overview*

348 Our study of the impact of wildfire smoke on inland waters found highly variable responses in
349 both GPP and R. On average, GPP and R were significantly lower on smoke days, but the
350 magnitude and direction of responses varied considerably among and within sites, and between
351 years. Median differences in GPP between non-smoke and smoke days ranged from +0.5 to - 0.9
352 mg DO L⁻¹ d⁻¹. Responses in R also varied but were more clearly linked to site characteristics
353 such as nutrient concentrations and water temperature. The average spatial extent of med-high
354 density smoke between June-October has increased to over 50% of California's area since 2006,
355 and smoke is associated with significant reductions in SW radiation and 3 to 4-fold increases in
356 atmospheric PM_{2.5}, suggesting widespread impacts to California's thousands of lakes, ponds,
357 and tidal freshwaters²⁵. These findings establish that metabolic responses of inland waters to
358 smoke, both in the western U.S. and globally, will be highly dependent on spatial and seasonal
359 context of smoke coverage as well as physical and chemical attributes of individual ecosystems.

360 *Multiple mechanisms drive lake metabolic responses to wildfire smoke*

361 We identify several mechanisms responsible for the variation in responses of ecosystem
362 metabolic rates to wildfire smoke. All sites were exposed to multiple weeks of high-density
363 smoke cover and reduced SW radiation fluxes (Table 2), yet GPP responses often differed in
364 magnitude and direction, even within the same site, underscoring the need to better understand
365 how changes in light affect aquatic primary producers in different habitats. In many of our
366 datasets, GPP did not change substantially during smoky periods, suggesting that primary
367 producers were neither strongly light-limited nor strongly photo-inhibited (Figure 1a). Lack of
368 strong light-limitation in our datasets is not surprising given that we only estimated GPP in

369 surface waters—Scordo et al.⁸ found that smoke cover increased GPP in surface waters but
370 inhibited GPP in deeper waters and prevented the seasonal formation of a deep chlorophyll
371 maximum⁸. In oligotrophic water bodies with deep chlorophyll maxima, smoke cover may
372 substantially reduce whole-lake GPP. However, we were surprised by the variable responses in
373 littoral habitats, where we expected minimal responses due to structural and physiological
374 adaptations by benthic algae to high-light (PAR and UV) conditions²⁶. Sensitivity of aquatic
375 primary producers to photo-inhibition has been shown to be highly taxon-specific²⁷, thus better
376 characterization of algal community composition may be required to understand smoke
377 responses in shallow or near-shore aquatic habitats.

378 Nutrient fertilization from smoke aerosol deposition can stimulate aquatic primary production,
379 especially in oligotrophic systems (Figure 1c)⁶. Phosphorus, a critical and often limiting nutrient
380 in freshwater ecosystems, is present in significantly higher concentrations in ash compared to the
381 unburned vegetation from which it originates²⁸. However, there are few studies examining the
382 fate of smoke particles in lakes and results are often ambiguous. Alpine lakes in proximity to
383 biomass burning exhibited increased P concentrations and subsequently N-limitation²⁹. In ultra-
384 oligotrophic Lake Tahoe, the addition of ash from smoke increased primary productivity relative
385 to a control treatment, yet no significant differences were found in time series of nitrate,
386 ammonium, or phosphate concentrations, leading the researchers to conclude that trace metals in
387 ash, rather than N or P, increased production¹⁶. Scordo et al.⁸ found that smoke increased
388 particulate N and C in a mesotrophic lake, but smoke did not change the type and level of
389 macronutrient limitation in bioassays. We did not measure nutrient concentrations at temporal
390 resolution sufficient to test hypotheses related to nutrient fertilization, but in lakes where GPP

391 was higher during smoke cover, it is plausible that nutrient fertilization may have stimulated
392 primary production.

393 Changes in light (e.g., UV radiation) and nutrients alter ecosystem respiration rates in
394 oligotrophic waters more so than productive waters³⁰. R decreased during smoke cover in all the
395 oligotrophic study lakes, even when GPP increased (Figure 4g, h). Reductions in UV radiation
396 during smoke cover should have greater effects on R in oligotrophic systems for two reasons.
397 First, UV irradiance is higher in clear-water oligotrophic waters and imposes substantial
398 energetic costs on aquatic organisms to repair cellular damage³¹, thus UV reduction during
399 smoke cover should decrease ecosystem respiration rates by decreasing energetic costs. Second,
400 reducing UV improves the quality (e.g., nutrient stoichiometry) of organic matter fixed by
401 autotrophs³², increasing bacterial growth efficiency and decreasing ecosystem respiration rates
402 in oligotrophic systems^{33,34}, where bacterioplankton account for the majority of respiration³⁵.
403 Moreover, though our study did not quantify changes in nutrient concentrations associated with
404 ash deposition, even mild fertilization in oligotrophic surface waters can increase C:N and C:P
405 ratios in autotrophic biomass, increasing bacterial growth efficiency and reducing R. Impacts of
406 prolonged smoke cover on carbon cycling and emissions from inland waters may depend equally
407 on the responses of primary producers and heterotrophs.

408 The seasonal timing of wildfire smoke cover is another important factor that mediates lake
409 ecosystem responses, particularly for GPP. The effects of PAR and UV reduction from smoke
410 should vary seasonally— smoke cover in early summer, when solar radiation inputs are at their
411 annual maximum, could stimulate GPP if phytoplankton are photo-inhibited, whereas smoke
412 cover in autumn, when PAR is declining, may further reduce GPP (Figure 1a). The effects of
413 nutrient fertilization from smoke should also vary seasonally in water bodies with strong

414 seasonal changes in nutrient limitation. For example, phytoplankton may be less nutrient-limited
415 in autumn when mixing and thermocline deepening replenish nutrient concentrations in surface
416 waters³⁶. Two of our study years (2020, 2021) had late-season smoke cover, with dense smoke
417 persisting through October (Figure 2b), which may have contributed to the overall reductions in
418 GPP with smoke cover that we observed. In contrast, sites where GPP increased during smoke
419 cover (Castle Lake pelagic in 2018, Lake Tahoe nearshore sites in 2021) had earlier exposure to
420 smoke, with a greater number of smoke days in July (Table 2). Though our study took place
421 during years with relatively late-season smoke cover, this pattern is not necessarily
422 representative of smoke exposure in California or elsewhere. Smoke covered at least 50% of
423 California during June in 7 out of 17 years (Supplementary Figure 1). The record-breaking 2023
424 Canadian wildfires began in May and early June, when solar radiation fluxes were highest, and
425 covered extensive, lake-rich regions in smoke for weeks³⁷. The high degree of variation in
426 seasonal timing of smoke cover implies that lake responses could change from year-to-year
427 depending on the timing of wildfire ignitions.

428 Predicting the impacts of worsening wildfire smoke on inland waters at regional to continental
429 scales requires understanding how lake and watershed attributes mediate lake responses. In
430 North America over a million lakes were exposed to smoke for over 30 days per year (2019-
431 2021)³, encompassing biomes from arctic to subtropical, and subsequently an enormous range in
432 water temperature, clarity, and nutrient concentrations. Our study sites ranged from ultra-
433 oligotrophic to hypereutrophic, and we observed correspondingly variable responses of lake GPP
434 and R to smoke cover. R in particular responded differently in warm, eutrophic lakes than in
435 cold, oligotrophic lakes (Figure 4h, 5c), whereas GPP responses were less clearly related to lake
436 trophic status. The small, oligotrophic mountain lakes in Sequoia National Park, which are

437 representative of a majority of California's lakes²⁵, experienced the greatest relative declines in R
438 during smoke cover and often increased NEP (Supplementary Table 1, Extended Data Figure 3),
439 suggesting that smoke may have regionally significant impacts on aquatic carbon cycling. In
440 other lake regions where eutrophication or high organic matter concentrations are prevalent,
441 smoke cover may lead to reduced NEP and greater CO₂ fluxes from lakes if GPP decreases but
442 respiration rates remain high.

443 Our results highlight the need for targeted research of smoke impacts on freshwaters, as a key set
444 of basic questions remain unresolved: 1) How do lake attributes such as water clarity, trophic
445 status, or lake size and depth mediate metabolic responses to smoke? 2) Do the mechanistic
446 relationships that determine responses of GPP and R to smoke cover vary among different
447 communities of autotrophs and heterotrophs? 3) How do attributes of smoke exposure mediate
448 lake responses? and 4) Does prolonged, dense smoke affect aquatic carbon cycling at regional or
449 global scales? We were unable to clearly distinguish the roles of smoke exposure attributes and
450 lake attributes in mediating metabolic responses to smoke, due to covariation in these factors and
451 the limited number of datasets in our study. Understanding lake responses to smoke will require
452 extensive data collection across different hydroclimatic conditions, environmental gradients
453 (geomorphology, vegetation, land use), and gradients in smoke exposure. Additional
454 experimental, empirical, and modeling studies are also needed to understand the predominant
455 mechanisms underlying whole-ecosystem metabolic responses to smoke. Even small impacts on
456 ecosystem metabolic rates may have important implications for global carbon cycling given the
457 large number of lakes affected by smoke globally³. Quantifying impacts of smoke on aquatic
458 carbon cycling at regional to continental scales will require collaborative research within and
459 across regions. Global-scale, opportunistic data collection by lake sensor networks such as the

460 Global Lake Ecological Observatory Network (GLEON; <https://gleon.org/>) could be used to test
461 hypotheses and broaden our understanding of this increasing global phenomenon, as wildfires
462 and smoke cover increase in frequency, intensity, and spatial extent.

463

464

465

466

467

468

469

470

471

472

473

474

475

476

477 **References**

- 478 1. Senande-Rivera, M., Insua-Costa, D. & Miguez-Macho, G. Spatial and temporal
479 expansion of global wildland fire activity in response to climate change. *Nat. Commun.*
480 **13**, (2022).
- 481 2. Baars, H. *et al.* Californian Wildfire Smoke Over Europe: A First Example of the Aerosol
482 Observing Capabilities of Aeolus Compared to Ground-Based Lidar. *Geophys. Res. Lett.*
483 **48**, (2021).
- 484 3. Farruggia, M. J. *et al.* Wildfire smoke impacts lake ecosystems. (2023).
485 doi:<https://doi.org/10.31223/X53H41>
- 486 4. McLauchlan, K. K. *et al.* Fire as a fundamental ecological process: Research advances and
487 frontiers. *J. Ecol.* **108**, 2047–2069 (2020).
- 488 5. Vicars, W. C., Sickman, J. O. & Ziemann, P. J. Atmospheric phosphorus deposition at a
489 montane site: Size distribution, effects of wildfire, and ecological implications. *Atmos.*
490 *Environ.* **44**, 2813–2821 (2010).
- 491 6. Tang, W. *et al.* Widespread phytoplankton blooms triggered by 2019–2020 Australian
492 wildfires. *Nature* **597**, 370–375 (2021).
- 493 7. David, A. T., Asarian, J. E. & Lake, F. K. Wildfire Smoke Cools Summer River and
494 Stream Water Temperatures. *Water Resour. Res.* **54**, 7273–7290 (2018).
- 495 8. Scordo, F. *et al.* Smoke from regional wildfires alters lake ecology. *Sci. Rep.* **11**, 1–14
496 (2021).

- 497 9. Allen, A. P., Gillooly, J. F. & Brown, J. H. Linking the global carbon cycle to individual
498 metabolism. *Funct. Ecol.* **19**, 202–213 (2005).
- 499 10. Rastogi, B. *et al.* Enhanced Photosynthesis and Transpiration in an Old Growth Forest
500 Due To Wildfire Smoke. *Geophys. Res. Lett.* **49**, 1–13 (2022).
- 501 11. Corwin, K. A., Corr, C. A., Burkhardt, J. & Fischer, E. V. Smoke-Driven Changes in
502 Photosynthetically Active Radiation During the U.S. Agricultural Growing Season. *J.*
503 *Geophys. Res. Atmos.* **127**, (2022).
- 504 12. Hemes, K. S., Verfaillie, J. & Baldocchi, D. D. Wildfire-Smoke Aerosols Lead to
505 Increased Light Use Efficiency Among Agricultural and Restored Wetland Land Uses in
506 California’s Central Valley. *J. Geophys. Res. Biogeosciences* **125**, 1–21 (2020).
- 507 13. Ardyna, M. *et al.* Wildfire aerosol deposition likely amplified a summertime Arctic
508 phytoplankton bloom. *Commun. Earth Environ.* **3**, 1–8 (2022).
- 509 14. Li, M., Shen, F. & Sun, X. 2019–2020 Australian bushfire air particulate pollution and
510 impact on the South Pacific Ocean. *Sci. Rep.* **11**, 1–13 (2021).
- 511 15. Scordo, F., Sadro, S., Culpepper, J., Seitz, C. & Chandra, S. Wildfire Smoke Effects on
512 Lake-Habitat Specific Metabolism: Toward a Conceptual Understanding. *Geophys. Res.*
513 *Lett.* **49**, 1–10 (2022).
- 514 16. Goldman, C. R., Jassby, A. D. & de Amezaga, E. Forest fires, atmospheric deposition and
515 primary productivity at Lake Tahoe, California-Nevada. *Int. Vereinigung für Theor. und*
516 *Angew. Limnol. Verhandlungen* **24**, 499–503 (1990).

- 517 17. Olson, N. E., Boaggio, K. L., Rice, R. B., Foley, K. M. & LeDuc, S. D. *Wildfires in the*
518 *western United States are mobilizing PM_{2.5}-associated nutrients and may be contributing*
519 *to downwind cyanobacteria blooms. Environmental Science: Processes and Impacts* **25**,
520 (2023).
- 521 18. Junghenn Noyes, K. T., Kahn, R. A., Limbacher, J. A. & Li, Z. Canadian and Alaskan
522 wildfire smoke particle properties, their evolution, and controlling factors, from satellite
523 observations. *Atmos. Chem. Phys.* **22**, 10267–10290 (2022).
- 524 19. Staehr, P. A. *et al.* The metabolism of aquatic ecosystems: History, applications, and
525 future challenges. *Aquat. Sci.* **74**, 15–29 (2012).
- 526 20. Kanniah, K. D., Beringer, J., North, P. & Hutley, L. Control of atmospheric particles on
527 diffuse radiation and terrestrial plant productivity: A review. *Prog. Phys. Geogr.* **36**, 209–
528 237 (2012).
- 529 21. Williams, A. P. *et al.* Observed Impacts of Anthropogenic Climate Change on Wildfire in
530 California. *Earth's Futur.* **7**, 892–910 (2019).
- 531 22. Cal Fire Incidents. (2023). Available at: <https://www.fire.ca.gov/incidents>. (Accessed: 1st
532 July 2023)
- 533 23. Solomon, C. T. *et al.* Ecosystem respiration: Drivers of daily variability and background
534 respiration in lakes around the globe. *Limnol. Oceanogr.* **58**, 849–866 (2013).
- 535 24. Smith, E. M. & Prairie, Y. T. Bacterial metabolism and growth efficiency in lakes: The
536 importance of phosphorus availability. *Limnol. Oceanogr.* **49**, 137–147 (2004).

- 537 25. Melack, J. M., Sadro, S., Sickman, J. O. & Dozier., J. *Lakes and watersheds in the Sierra*
538 *Nevada of California: Responses to environmental change*. (Univ. Calif. Press., 2021).
- 539 26. Vinebrooke, R. D. & Leavitt, P. R. Differential Responses of Littoral Communities to
540 Ultraviolet Radiation in an Alpine Lake. *Ecology* **80**, 223 (1999).
- 541 27. Vincent, W. F. & Roy, S. Solar ultraviolet-B radiation and aquatic primary production:
542 damage, protection, and recovery. *Environ. Rev.* **1**, 1–12 (1993).
- 543 28. Raison, R. J., Khanna, P. K. & Woods, P. V. Transfer of elements to the atmosphere
544 during low-intensity prescribed fires in three Australian subalpine eucalypt forests. *Can. J.*
545 *For. Res.* **15**, 657–664 (1985).
- 546 29. Brahney, J., Mahowald, N., Ward, D. S., Ballantyne, A. P. & Neff, J. C. Is atmospheric
547 phosphorus pollution altering global alpine lake stoichiometry? *Global Biogeochem.*
548 *Cycles* 1369–1383 (2015). doi:doi:10.1002/2015GB005137
- 549 30. Roberts, B. J. & Howarth, R. W. Nutrient and light availability regulate the relative
550 contribution of autotrophs and heterotrophs to respiration in freshwater pelagic
551 ecosystems. *Limnol. Oceanogr.* **51**, 288–298 (2006).
- 552 31. Williamson, C. E. & Zagarese, H. E. The impact of UV-B radiation on pelagic freshwater
553 ecosystems. in *Advances in Limnology* (1994).
- 554 32. Harrison, J. W. & Smith, R. E. H. Effects of ultraviolet radiation on the productivity and
555 composition of freshwater phytoplankton communities. *Photochem. Photobiol. Sci.* **8**,
556 1218–1232 (2009).

- 557 33. Tranvik, L. J. & Bertilsson, S. Contrasting effects of solar UV radiation on dissolved
558 organic sources for bacterial growth. *Ecol. Lett.* **4**, 458–463 (2001).
- 559 34. Sadro, S., Nelson, C. E. & Melack, J. M. Linking diel patterns in community respiration
560 to bacterioplankton in an oligotrophic high-elevation lake. *Limnol. Oceanogr.* **56**, 540–
561 550 (2011).
- 562 35. Biddanda, B., Ogdahl, M. & Cotner, J. Dominance of bacterial metabolism in oligotrophic
563 relative to eutrophic waters. *Limnol. Oceanogr.* **46**, 730–739 (2001).
- 564 36. Sadro, S., Melack, J. M. & MacIntyre, S. Depth-integrated estimates of ecosystem
565 metabolism in a high-elevation lake (Emerald Lake, Sierra Nevada, California). *Limnol.*
566 *Oceanogr.* **56**, 1764–1780 (2011).
- 567 37. Dong, M. *et al.* Maps: Tracking Air Quality and Smoke From Wildfires. (2023). Available
568 at: [https://www.nytimes.com/interactive/2023/us/smoke-maps-canada-](https://www.nytimes.com/interactive/2023/us/smoke-maps-canada-fires.html?searchResultPosition=14)
569 [fires.html?searchResultPosition=14](https://www.nytimes.com/interactive/2023/us/smoke-maps-canada-fires.html?searchResultPosition=14).
- 570 38. Hazard Mapping System Fire and Smoke Product. (2023). Available at:
571 <https://www.ospo.noaa.gov/Products/land/hms.html#stats-smoke>. (Accessed: 1st July
572 2023)
- 573 39. Jassby, A. D. & Cloern, J. E. wq: Exploring water quality monitoring data. (2022).
- 574 40. Wildlife, C. D. of F. and. California Lake Database. (2022). Available at: [https://data-](https://data-cdfw.opendata.arcgis.com/datasets/CDFW::california-lakes)
575 [cdfw.opendata.arcgis.com/datasets/CDFW::california-lakes](https://data-cdfw.opendata.arcgis.com/datasets/CDFW::california-lakes).
- 576 41. Meyers, B., Tabone, M. & Kara, E. C. *Statistical clear sky fitting algorithm*. (2019).

577 doi:arXiv:1907.08279

- 578 42. Winslow, L. A. *et al.* LakeMetabolizer: An R package for estimating lake metabolism
579 from free-water oxygen using diverse statistical models. *Inl. Waters* **6**, 622–636 (2016).
- 580 43. Read, J. S. *et al.* Derivation of lake mixing and stratification indices from high-resolution
581 lake buoy data. *Environ. Model. Softw.* **26**, 1325–1336 (2011).
- 582 44. Vachon, D. & Prairie, Y. T. The ecosystem size and shape dependence of gas transfer
583 velocity versus wind speed relationships in lakes. *Can. J. Fish. Aquat. Sci.* **70**, 1757–1764
584 (2013).
- 585 45. Staehr, P. A., Brighenti, L. S., Honti, M., Christensen, J. & Rose, K. C. Global patterns of
586 light saturation and photoinhibition of lake primary production. *Inl. Waters* **6**, 593–607
587 (2016).
- 588 46. Wood, S. N. Fast stable restricted maximum likelihood and marginal likelihood estimation
589 of semiparametric generalized linear models. *J. R. Stat. Soc. Ser. B Stat. Methodol.* **73**, 3–
590 36 (2011).

591

592

593

594

595

596 **Acknowledgements**

597 APS and AC were supported by NSF RAPID Award # 2102344 to SS, YJ, and GS. MJF was
598 supported by NSF GRFP Award # 2036201. SAV and SW were supported by the Tahoe
599 Regional Planning Agency and the Lahontan Regional Water Quality Control Board.

600 **Author Contributions**

601 APS, FS and SS designed the study. APS, MJF, AC, FS, SC, MT, JC, GS, SAV, and SW
602 provided datasets. APS, MT, FS, AC, JC, and SS performed data analyses and made the figures.
603 APS lead manuscript writing. All authors contributed text and edited the manuscript.

604

605

606

607

608

609

610

611

612

613 **Tables**

614 **Table 1.** Study site locations and attributes.

Site Name	CA Region	Latitude (°)	Longitude (°)	Elevation (m.a.s.l)	Surface Area (ha)	Max Depth (m)	Chl-a ($\mu\text{g L}^{-1}$)	Light Attenuation (k_d, m^{-1})	Study Periods
Delta	Sacramento-San Joaquin River Delta	38.48	-121.585	0	1,160	10	4.8 (3.4)	1.58	8/1/2020 - 11/1/2020
Clear Lake	N. Coast Range	39.064	-122.842	431	15,100	8	17.5 (9.4) LA ¹ 59.5 (38.1) OA ²	0.8	7/1/2020-11/1/2020
Dulzura Lake (Tahoe) ³	N. Sierra Nevada	39.298	-120.383	2,097	14.8	9.5	1.6 (1.1)	0.53	7/1/2021 - 10/1/2021
Castle Lake	Klamath	41.227	-122.383	1,646	20.1	30	0.79 (0.25)	0.25	7/1/2018 - 10/1/2018
TOK 11 Pond (Sequoia)	S. Sierra Nevada	36.594	-118.671	2,970	0.2	2.3	0.65 (0.60)	0.22	7/1/2020 - 11/1/2020; 7/1/2021-11/1/2021
EML Pond 1 (Sequoia)	S. Sierra Nevada	36.599	-118.679	2,802	0.2	3.1	0.88 (0.49)	0.22	7/1/2020 - 11/1/2020; 7/1/2021-11/1/2021
Topaz Pond (Sequoia)	S. Sierra Nevada	36.625	-118.635	3,229	0.2	1.9	0.86 (1.04)	0.22	7/1/2020 - 11/1/2020; 7/1/2021-11/1/2021
Topaz Lake (Sequoia)	S. Sierra Nevada	36.626	-118.637	3,219	3.8	5	1.44 (0.37)	0.22	7/1/2020 - 11/1/2020; 7/1/2021-11/1/2021
Emerald Lake (Sequoia)	S. Sierra Nevada	36.598	-118.676	2,800	2.8	10	0.74 (0.42)	0.24	7/1/2020 - 11/1/2020; 7/1/2021-11/1/2021
Lake Tahoe (Tahoe)	N. Sierra Nevada	39.103	-120.035	1,897	49,624	501	0.31 (0.13)	0.09	7/1/2020-11/1/2020; 7/1/2021 - 11/1/2021

¹ LA = Lower Arm

² OA = Oaks Arm

³ Names of groups of lakes corresponding to names shown in Figure 2 are included in parentheses

615 **Table 2.** Attributes of smoke exposure for selected study sites⁴.

Site	Year	# Smoke Days				# Consecutive Smoke Days		Mean PM2.5 (ug m ⁻³)	Mean SW _{diff} (W m ⁻²)	Cum. SW Deficit (10 ⁶ J m ⁻²)
		Tot	Jul	Aug	Sept	Mean	Max			
Lake Tahoe	2021	45	9	23	13	3	10	67	67	260.57
Emerald Lake	2021	38	4	13	20	4	20	79	79	259.62
Emerald Lake	2020	39	0	10	28	8	21	NA	59	199.59
Dulzura Lake	2021	36	9	20	7	3	9	55	55	169.73
Clear Lake	2020	30	0	12	17	3	7	60	60	154.38
Delta	2020	34	1	13	19	4	12	50	50	145.53
Lake Tahoe	2020	28	1	12	15	3	9	59	59	143.30
Clear Lake	2021	23	1	16	6	3	5	50	50	99.35
Castle Lake	2018	26	6	12	8	3	4	43	44	97.87

616

617

618

619

620

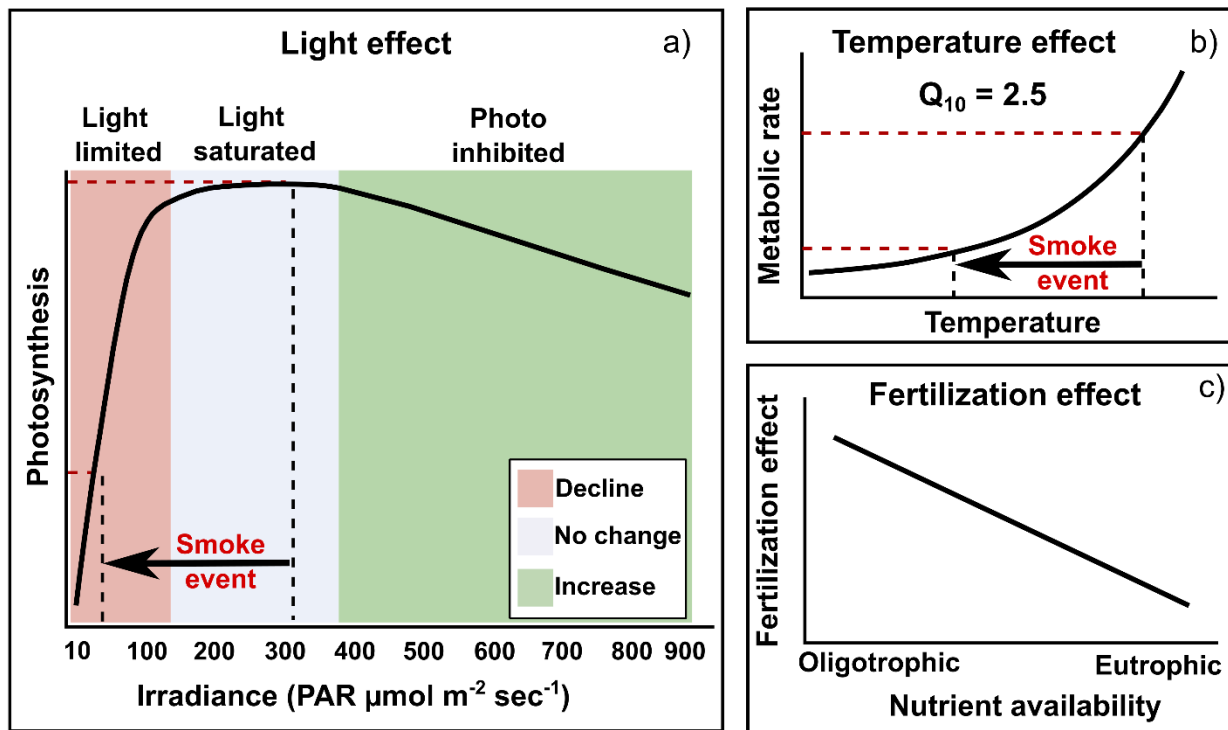
621

622

623 **Figures**

⁴ Smoke attributes were calculated for the period between June 1 – October 1 because some datasets were incomplete outside this range. Mean PM2.5 and SW_{diff} refer to means on smoke days only. Sites in close proximity (e.g., small lakes and ponds in Sequoia National Park) are not shown because they lacked unique meteorological datasets.

624 **Figure 1.** Smoke can affect aquatic ecosystem metabolism by multiple mechanisms. A) Smoke
 625 events (black horizontal arrow) reduce light (PAR) within the water column. Whether a smoke
 626 event increases or decreases GPP (colored regions) depends on the pre-smoke PAR level and on
 627 the magnitude of PAR reduction (e.g., smoke density). In this example, a smoke event reduces
 628 GPP because primary producers shift from light-saturated to light-limited conditions. B) Smoke
 629 events (black arrow) can reduce water temperature by scattering or absorbing incoming solar
 630 radiation, which should decrease metabolic rates (both GPP and R). C) The degree to which
 631 nutrient fertilization from smoke particle deposition stimulates GPP depends on ambient nutrient
 632 availability within a water body.

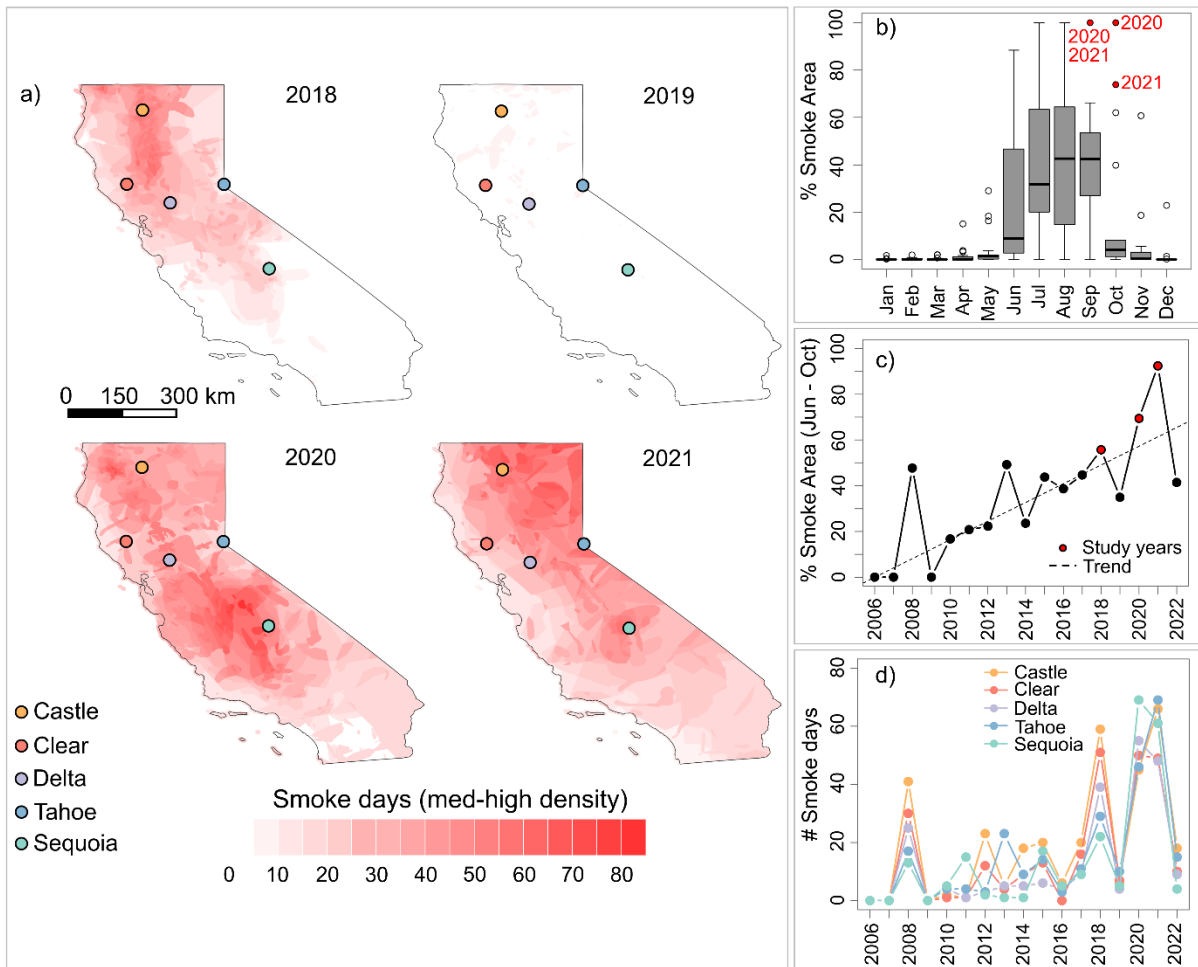


633

634

635 **Figure 2.** Spatial and temporal patterns in smoke cover in California (CA) and at study sites
 636 between 2006 - 2022. A) Maps show sites (colored dots) and the annual number of days with

637 med-high density smoke cover from 2018 – 2021 (red color gradient). Sites that are close
 638 together (ex. 5 lakes and ponds in Sequoia NP, multiple locations within the same lake) are
 639 represented by a single point. B) Seasonality of maximum spatial extent of med-high density
 640 smoke (percentage of CA; 2006-2022). September and October of 2020 and 2021 were outliers
 641 with high smoke cover extent. C) Average percentage of CA covered by med-high density
 642 smoke during June-October. Study years are shown in red, the dashed line shows the significant
 643 linear trend through time. D) Time series of total annual days with med-high density smoke
 644 cover at study sites from 2006-2022.



645

646

647

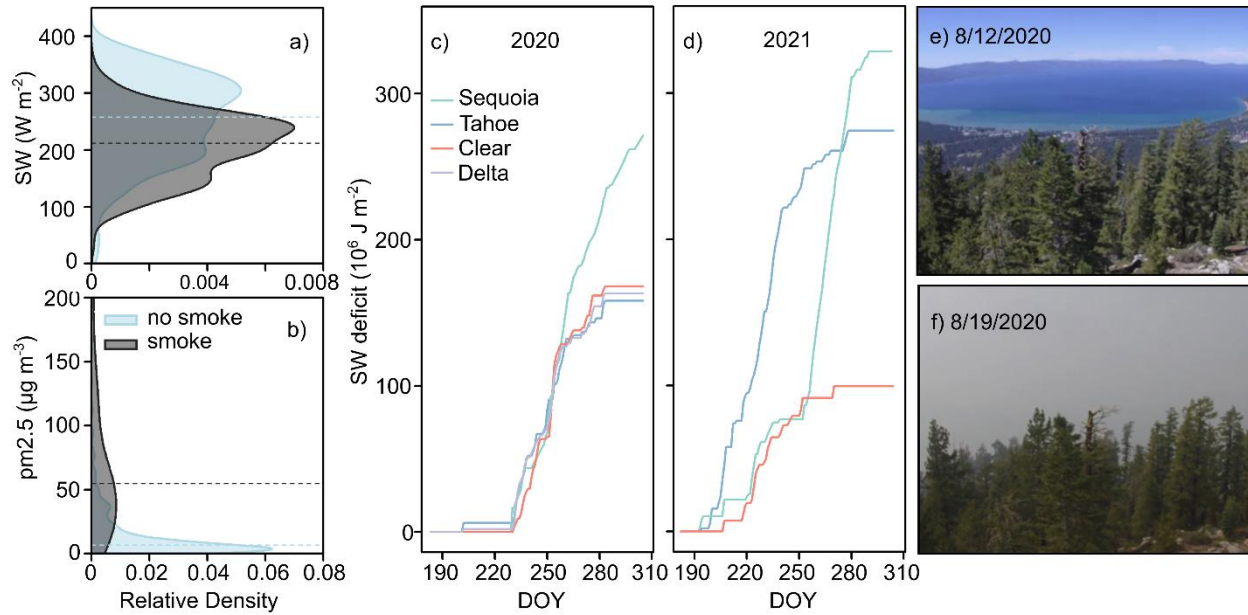
648

649

650

651

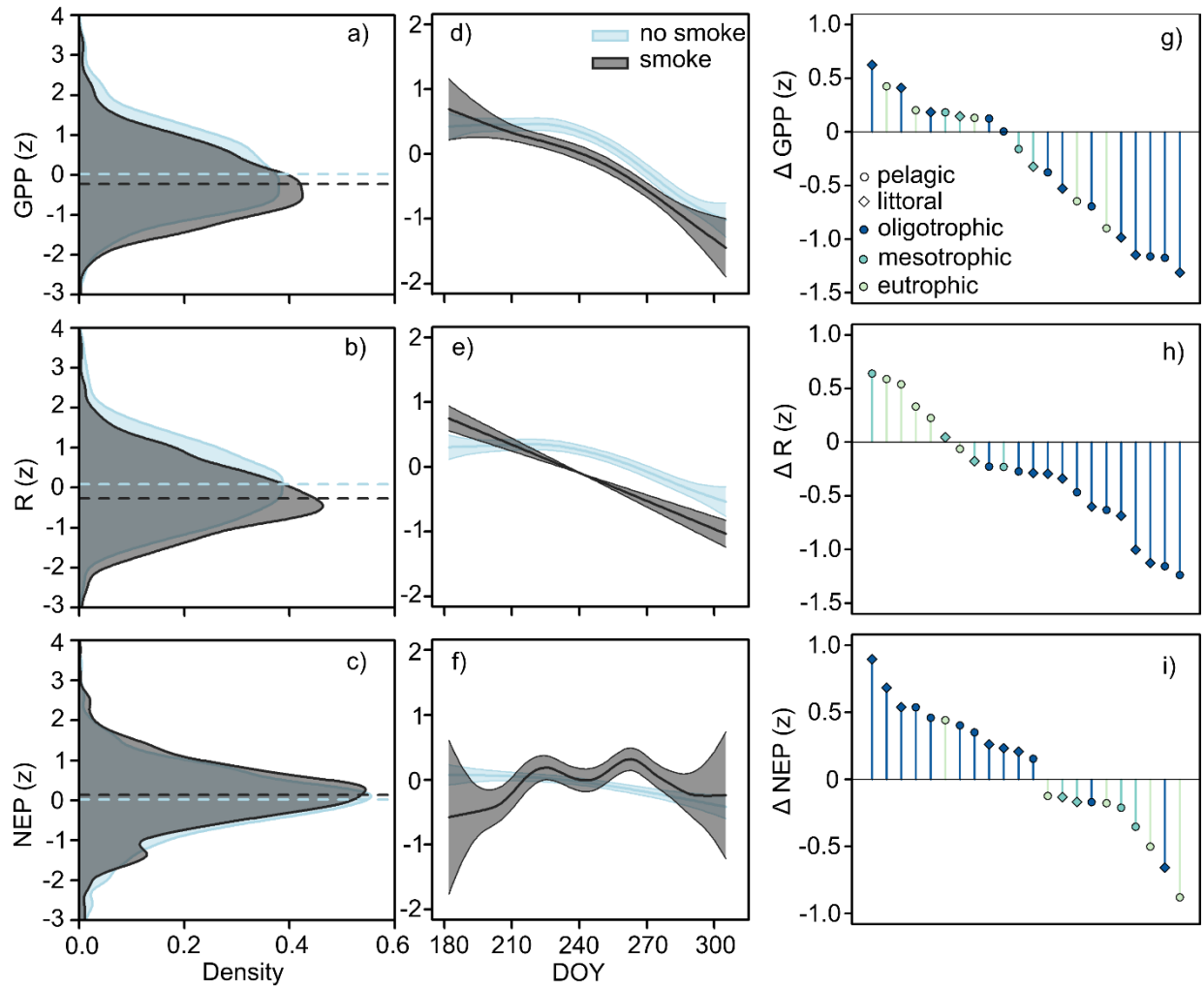
652 **Figure 3.** Changes in SW radiation and PM2.5 concentration during smoke cover. Density plots
653 of A) daily average SW radiation and B) daily average PM2.5 concentration on non-smoke (n =
654 694; blue) and smoke (n = 349; gray) days. Dashed horizontal lines show median values across 9
655 unique meteorological datasets. C - D) The cumulative deficit of SW radiation due to smoke
656 cover from July 1 (doy 183) to Nov 1 (doy 306) in 2020 and 2021 at our study sites. Horizontal
657 sections of the lines represent non-smoke days, vertical sections represent smoke events. E-F)
658 View of Lake Tahoe on 8/12/2020 at 14:00 PST (daily mean SW in Lake Tahoe = 340 W m^{-2} ,
659 $\text{PM}_{2.5} = 2.3 \mu\text{g m}^{-3}$), and a week later on 8/19/2020 14:00 PST, with view obscured by thick
660 smoke ($\text{SW} = 214 \text{ W m}^{-2}$; $\text{PM}_{2.5} = 114 \mu\text{g m}^{-3}$). Images were downloaded from
661 <http://ecam.cmucreatelab.org/embeds/tahoe2> (Heavenly). Notes: For clarity, some datasets that
662 are geographically proximate have been omitted from panels C-D. Castle Lake's cumulative SW
663 deficit is not shown because only data from 2018 were available. Data were not collected from
664 the Delta in 2021.



665

666

667 **Figure 4.** Responses of aquatic ecosystem metabolism to smoke cover. Density plots of A) daily
 668 z-scored GPP, B) R, and C) NEP on non-smoke (blue) and smoke (gray) days (n=1772). Dashed
 669 horizontal lines show the median values across 22 metabolism datasets. GAMM model smooth
 670 terms fit to day-of-year (DOY) showing how smoke cover alters seasonal trends in D) GPP, E)
 671 R, and F) NEP. Shaded areas show one standard error from the predicted line. Metabolism
 672 estimates were z-scored to facilitate comparison across datasets. G-I) The difference between
 673 median GPP, R, or NEP on smoke days versus non-smoke days (Δ GPP, R, NEP) for each dataset
 674 (n=22), ordered from most positive to most negative along the x-axis. Circles represent pelagic
 675 sites; diamonds represent littoral sites. Points and segments are colored by lake trophic status
 676 (oligotrophic=blue, mesotrophic=green, eutrophic=yellow).



677

678

679

680

681

682

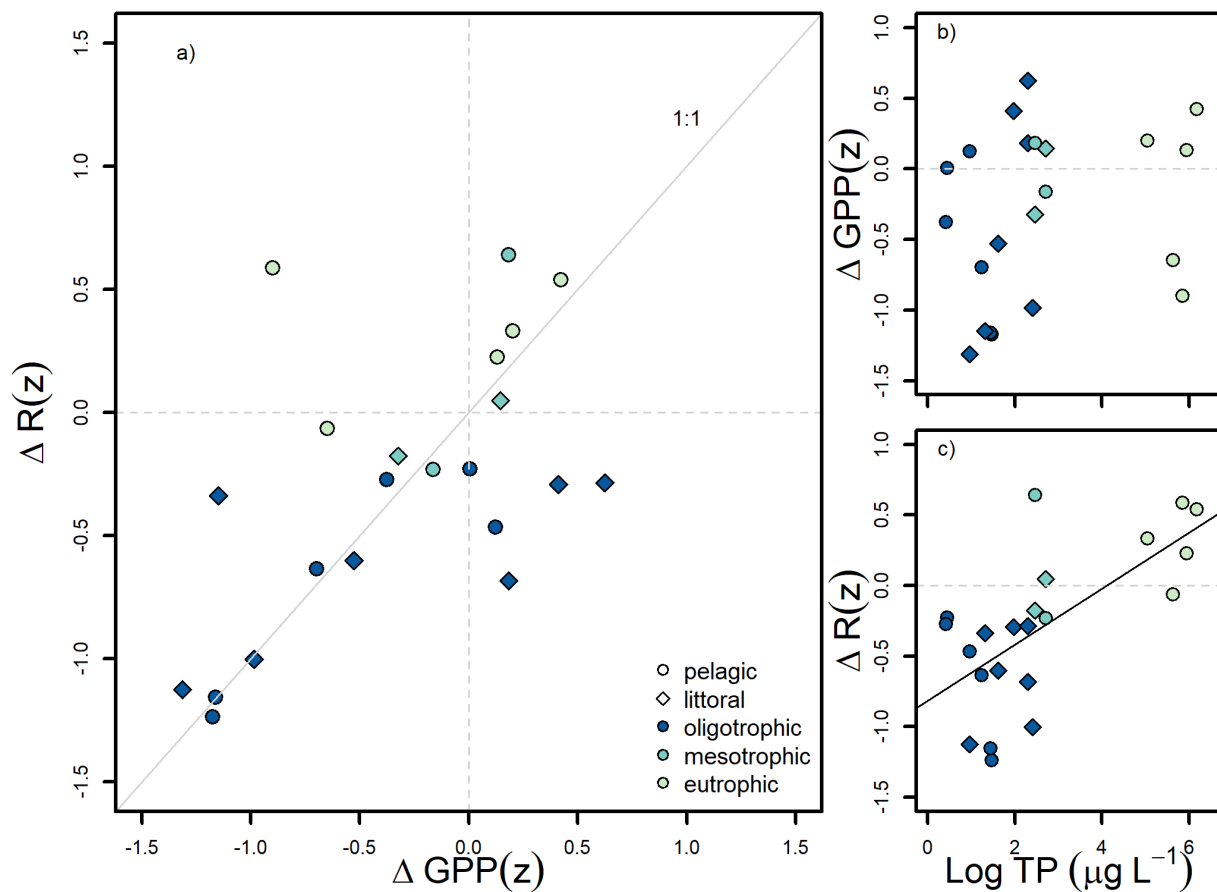
683

684

685

686 **Figure 5.** Coupling between responses of GPP and R to smoke and associations with nutrient
687 concentrations. A) For each dataset ($n = 22$) the median response of respiration to smoke (ΔR ; z-
688 scored; y-axis) is plotted against the median response of primary production (ΔGPP ; z-scored; x-
689 axis). Dashed horizontal and vertical lines show zero response, the gray diagonal line shows the
690 1:1 relationship. Circles represent pelagic sites; diamonds represent littoral sites. Points are
691 colored by lake trophic status as in Figure 4. B) ΔGPP (z-score) plotted against mean total
692 dissolved P (log TP; μL^{-1}). C) ΔR (z-score) plotted against log TP. The solid black line shows a
693 significant linear relationship ($R^2 = 0.41$, $p < 0.001$).

694



695

696

697